

a vesicle. The relationship between entry pressure, permeation pressure, and the deformability, size, and adhesion energy of a colloidal particle in an arbitrary pore is however still poorly understood.

are cylindrical coordinates about a system whose origin is at the center of the pore. The global equilibrium of the vesicle can be easily derived by taking the difference between μ_1 and μ_2 in order to obtain

$$P = 2 \gamma (\cos \theta_2 - \cos \theta_1). \tag{2}$$

Note that this expression is only valid for equilibrium or quasistatic systems in which the inner vesicle pressure is homogeneous and there is no fluid flow around the pore. A dynamic approach would require solving the Navier-Stokes equations coupled with the membrane governing equations [43]. By simple geometrical relations, one can show that the cap curvatures can be related to the pore geometry by $\frac{1}{r_i} \cos(\theta_i) = \frac{dr/dz}{r_i}$, where r_i and $\theta_i = \arctan[r'(z_i)]$ are the radii and the signed tangent angle (with dr/dz) of each contact line (Fig.1). Using the Young-Dupre relation [41], the contact angle can further be related to the adhesion energy between the vesicle and the pore by $\cos(\theta_i) = \frac{\gamma_{sv} - \gamma_{sl}}{\gamma}$, allowing us to express the cap curvatures in terms of the surface energy as

$$\frac{1}{r_i} \cos \theta_i = \frac{\gamma_{sv} - \gamma_{sl}}{\gamma} + \sin \theta_i \sqrt{1 - \cos^2 \theta_i}. \tag{3}$$

This relation, together with Eq.2, can be used to compute the pressure drop across a vesicle in a pore, as long as one knows the position of the contact lines x_1 and x_2 . It can be useful, for instance, to characterize the tendency of a vesicle to enter a pore by measuring its sudden pressure drop as it first makes contact with the pore surface. At this point, the two contact lines are confounded (i.e., $r_2 = r_1$ and $\theta_2 = \theta_1$) and we are left with the term $P = 4 \gamma \sin(\theta_1) \frac{\gamma_{sv} - \gamma_{sl}}{\gamma} \sqrt{1 - \cos^2 \theta_1}$, which measures the suction pressure that drives a vesicle into the pore. A simple observation of this equation shows that this pressure increases with adhesion energy and pore orientation angle θ_1 but decreases with the contact line radius

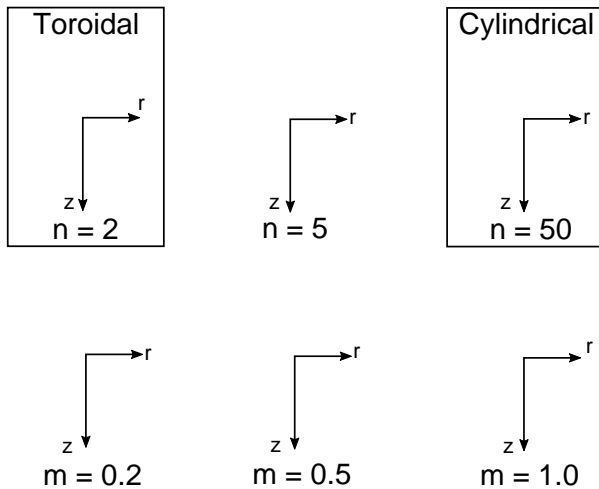
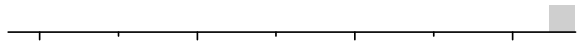
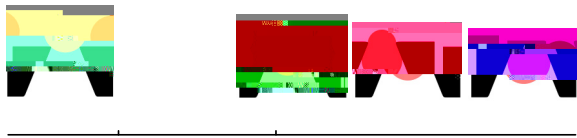


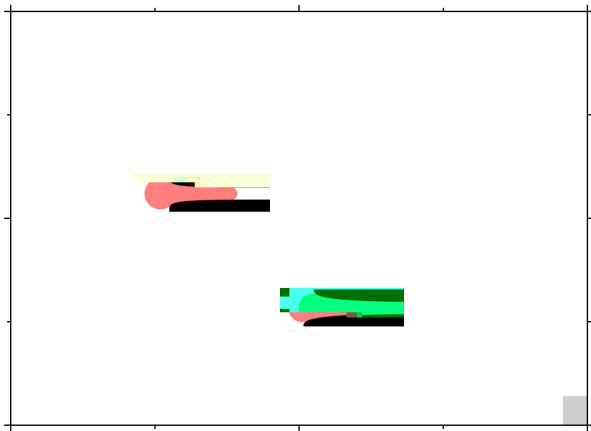
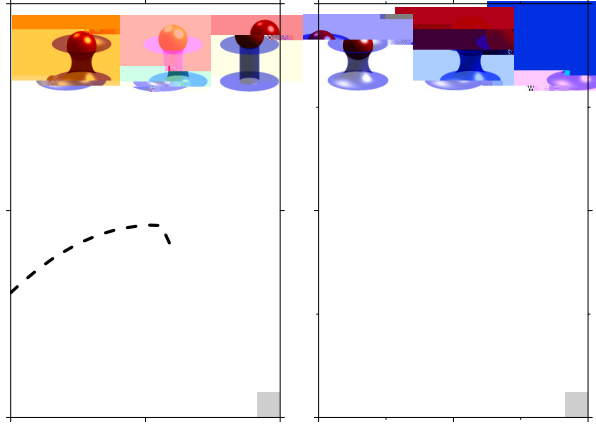
FIG. 2. Three-dimensional representation of the axisymmetric pore. In the top three figures, the values of n is kept constant at 0 while we vary the sharpness parameter m in the bottom figures is constant and equal to 5 while n is varied.

pronounced conical shapes are obtained as the magnitude of m increases; Eq. (8) can be used into the system of (5) and (6) to obtain an explicit form of the governing equations and a numerical solution for a variety of pore-vesicle systems (details are provided in Appendix).

A. Equilibrium diagrams

The equilibrium states of a soft vesicle confined in a pore can be visualized by the pressure diagram, showing the position of the center of mass of the vesicle in terms of the pressure drop P across the pore. Figures 3(a) and 3(b) show such diagrams for a normalized radius $R_s = 1.5$, adhesion energy $\gamma = 0$, and toroidal and cylindrical pore geometries. It can be seen that for symmetric pores ($\alpha = 0$) and nonwetting vesicles (solid lines), the diagram possesses three distinct regions (ascending, descending, and ascending), delimited in order by the maximum and the minimum values of the pressure drop P . The first region starts when the vesicle is tangent







and trapping efficiency is nonlinear and exhibits an optimum. (ii) The optimal design is a slightly tapered (moderate) conical shape. Indeed, we found that pronounced conical shapes (larger) would lose their asymmetric power by providing an overly restrictive pore opening. (iii) Trapping efficiency is promoted by larger pore curvatures, controlled by the shape parameter. Figure 8(c) further shows that the mechanics of asymmetric trapping is strongly affected by adhesion. This observation can be explained by the fact that the CPP is dominated by the XP, which involves mechanisms very

- [46] M. Szwast, T. Suchecka, and W. Kijwicz, *Chem. Process Eng.* **33**, 385 (2012).
- [47] C. Dekker, *Nat. Nanotechnol.* **2**, 209 (2007).
- [48] R. M. Hochmuth, *J. Biomech.* **33**, 15 (2000).
- [49] D. G. Hunter and B. J. Frisken, *Biophys. J.* **74**, 2996 (1998).
- [50] T. Darvishzadeh and N. V. Priezjev, *Membr. Sci.* **423-424**, 468 (2012).
- [51] L. Gorre, E. Ioannidis, and P. Silberzahn, *Europhys. Lett.* **33**, 267 (1996).
- [52] Q. Guo, S. M. McFaul, and H. Ma, *Phys. Rev. E* **83**, 051910 (2011).
- [53] T. F. Headen, S. M. Clarke, A. Perdigon, G. H. Meeten, J. D. Sherwood, and M. Aston, *J. Phys. Chem. C* **114**, 2997 (2010).